Development 134, 723-734 (2007) doi:10.1242/dev.02765

Fibroblast growth factor receptor 2 tyrosine kinase is required for prostatic morphogenesis and the acquisition of strict androgen dependency for adult tissue homeostasis

Yongshun Lin[1], Guoqin Liu[2], Yongyou Zhang[1], Ya-Ping Hu[3], Kai Yu[4], Chunhong Lin[1], Kerstin McKeehan[1], Jim W. Xuan[5], David M. Ornitz[4], Michael M. Shen[2], Norman Greenberg[6], Wallace L. McKeehan[1] and Fen Wang[1,*]

The fibroblast growth factor (FGF) family consists of 22 members and regulates a broad spectrum of biological activities by activating diverse isotypes of FGF receptor tyrosine kinases (FGFRs). Among the FGFs, FGF7 and FGF10 have been implicated in the regulation of prostate development and prostate tissue homeostasis by signaling through the FGFR2 isoform. Using conditional gene ablation with the Cre-LoxP system in mice, we demonstrate a tissue-specific requirement for FGFR2 in urogenital epithelial cells – the precursors of prostatic epithelial cells – for prostatic branching morphogenesis and prostatic growth. Most *Fgfr2* conditional null (*Fgfr2^{cn}*) embryos developed only two dorsal prostatic (dp) and two lateral prostatic (lp) lobes. This contrasts to wild-type prostate, which has two anterior prostatic (ap), two dp, two lp and two ventral prostatic (vp) lobes. Unlike wild-type prostates, which are composed of well developed epithelial ductal networks, the *Fgfr2^{cn}* prostates, despite retaining a compartmented tissue structure, exhibited a primitive epithelial architecture. Moreover, although *Fgfr2^{cn}* prostates continued to produce secretory proteins in an androgen-dependent manner, they responded poorly to androgen with respect to tissue homeostasis. The results demonstrate that FGFR2 is important for prostate organogenesis and for the prostate to develop into a strictly androgen-dependent organ with respect to tissue homeostasis but not to the secretory function, implying that androgens may regulate tissue homeostasis and tissue function differently. Therefore, *Fgfr2^{cn}* prostates provide a useful animal model for scrutinizing molecular mechanisms by which androgens regulate prostate growth, homeostasis and function, and may yield clues as to how advanced-tumor prostate cells escape strict androgen regulations.

KEY WORDS: Growth factor, Receptor tyrosine kinase, Androgen dependency, Prostate development, Mouse

INTRODUCTION

Development of mouse prostates is initiated at embryonic day 17 (E17) when a group of urogenital sinus epithelial cells derived from the hindgut endoderm grow out into the surrounding urogenital sinus mesenchyme in anterior, ventral, dorsal and lateral directions. These buds subsequently form the anterior, ventral, dorsal and lateral prostate lobes, respectively (Cunha et al., 2004; Thomson, 2001). At postnatal day 1 (P1), solid prostatic buds are formed surrounding the urethra. These buds already exhibit secondary and tertiary ductal branches. The ducts then undergo extensive branching morphogenesis, elongate from distal points and form intraductal mucosal infolding. Approximately 80% of ductal branching is completed by day 10 of neonatal life in mice, and the whole process is normally completed in 60-90 days. During the developmental stage, the epithelial cells differentiate into luminal secretory epithelial cells, basal epithelial cells and neuroendocrine cells, concurrent with the differentiation of mesenchyme into smooth muscle cells and fibroblasts (Cunha et al., 2004; Hayward et al., 1997).

[1]Center for Cancer Biology and Nutrition, Institute of Biosciences and Technology, Texas A&M Health Science Center, 2121 W. Holcombe Blvd, Houston, TX 77030-3303, USA. [2]State Key Laboratory of Plant Physiology and Biochemistry, College of Biological Sciences, China Agricultural University, Beijing 100094, P.R. China. [3]Center for Advanced Biotechnology and Medicine, UMDNJ-Robert Wood Johnson Medical School, 679 Hoes Lane, Piscataway, NJ 08854, USA. [4]Department of Molecular Biology and Pharmacology, Washington University, School of Medicine, 660 South Euclid Avenue, St Louis, MO, 63110, USA. [5]Department of Surgery, University of Western Ontario, London, ON, N6A 4G5, Canada. [6]Clinical Research Division, Fred Hutchinson Cancer Research Center, 1100 Fairview Avenue, Seattle, WA 98109-1024, USA.

*Author for correspondence (e-mail: fwang@ibt.tmc.edu)

Accepted 29 November 2006

Adult prostates are androgen-dependent organs with respect to growth, tissue homeostasis and function. Normally, the epithelium rapidly regresses to an atrophic state upon depletion of androgens. Approximately 35% of the ductal tips and branch-points are lost in distal regions within 2 weeks after orchiectomy. Androgen replenishment induces active cellular proliferation in the epithelium of atrophied prostate within 2 days, and the epithelial ducts completely regenerate within 14 days (Sugimura et al., 1986b). Because tissue-recombination experiments showed that the androgen receptor (AR) in epithelial cells is not essential for prostates to respond to androgens, it is proposed that paracrinal growth factors between stromal and epithelial compartments mediate at least some of the regulatory functions of androgen, and are crucial for androgens to instruct epithelial cells undergoing proliferation and differentiation (Cunha, 1996; Cunha et al., 2004; McKeehan et al., 1998; Thomson, 2001). Reciprocal communication from epithelia to mesenchyme may also play similar roles in stroma development, particularly in the differentiation to smooth muscle cells (Cunha, 1994; Cunha et al., 1996; Cunha et al., 2004; Hayward et al., 1998; Jin et al., 2004). It remains unresolved whether androgens regulate growth, tissue homeostasis and tissue functions via similar signaling mechanisms, although the FGF signaling axis has been implicated to be important for androgen signaling in prostates.

The mammalian FGF family consists of at least 22 gene products that control a wide spectrum of cellular processes. Most FGFs bind and activate transmembrane tyrosine kinases receptors (FGFRs) encoded by four highly conserved genes that exhibit a variety of splice variants (McKeehan et al., 1998; Powers et al., 2000; Wang and McKeehan, 2003). Expression of FGFs and FGFRs is spatiotemporally-specific in embryos and tissue- and cell-type-

specific in adults. Aberrant activations of FGF signaling pathways are found in developmental disorders and in diverse adult-tissue-specific pathologies, including malignant cancer (McIntosh et al., 2000; McKeehan et al., 1998; Ornitz, 2000; Wang and McKeehan, 2003).

In prostate, members of the FGF family and alternative splice forms of FGFRs are partitioned in the epithelium and mesenchyme (stroma), mediating directional and reciprocal communications between the two compartments. Ablation of this two-way communication in mature prostates perturbs tissue homeostasis and leads to prostatic intraepithelial neoplasia (PIN) and progressively more-severe lesions (Jin et al., 2003a; McKeehan et al., 1998). In addition, a series of stepwise changes in FGF signaling contributes to the progression of prostate lesions, including a reduction in resident FGFR2 expression accompanied by the expression of ectopic epithelial FGFR1 (Jin et al., 2003a; Kwabi-Addo et al., 2001; Lu et al., 1999; McKeehan et al., 1998; Pirtskhalaishvili and Nelson, 2000). Additionally, changes in the expression of FGF1, FGF2 (Ropiquet et al., 1999), FGF6 (Ropiquet et al., 2000), FGF8 (Dorkin et al., 1999; Gnanapragasam et al., 2002; Song et al., 2002; Wang et al., 1999), FGF9 (Giri et al., 1999b) and FGF17 (Polnaszek et al., 2004) have been observed to be associated with prostatic lesions.

During prostatic organogenesis, messenger mRNAs for both FGF7 and FGF10 are localized in the mesenchyme, and the receptors for FGF7 or FGF10 are found in the epithelium of the urogenital sinus in embryos and in the distal signaling center of elongating and branching ducts in postnatal prostates (Huang et al., 2005; Thomson and Cunha, 1999). Both FGF7 and FGF10 can substitute for androgens in organ culture of neonatal prostates, supporting extensive epithelial growth and ductal-branching morphogenesis. Ablation of *Fgf10* alleles abrogates prostate development and diminishes androgen responsiveness of prostatic rudiments in organ-culture and tissue-recombination experiments (Donjacour et al., 2003). This suggests that FGF10 signaling is essential for prostate development. Although it is generally accepted that the FGFR2IIIb isoform is the primary receptor for FGF10, the inability of mice deficient in FGFR2 to survive has prevented a direct analysis of the function of FGFR2 in prostate development, maintenance of homeostasis and androgen dependency.

To overcome this limitation, we specifically disrupted *Fgfr2* alleles in prostate precursor cells at E17.5. Unlike normal prostates, which are composed of two anterior, two dorsal, two lateral and two ventral lobes, most young-adult $Fgfr2^{cn}$ mice developed a small prostate that was frequently limited to two dorsal and two lateral lobes. Development of the epithelial compartment *in* $Fgfr2^{cn}$ prostates was impaired, which could be characterized by a deficiency in intralumenal infolding. In contrast to wild-type prostates, maintenance of mature $Fgfr2^{cn}$ prostates was not strictly androgen dependent. No significant prostatic atrophy was observed 2 weeks after castration in adult $Fgfr2^{cn}$ mice. Similarly, androgen replenishment to the castrated males also failed to induce cell proliferation in $Fgfr2^{cn}$ prostates. The results showed that FGFR2 signals were essential for strict androgen dependency in adult prostates with respect to tissue homeostasis. Interestingly, as in control prostates, the production of secretory proteins in $Fgfr2^{cn}$ prostates was dramatically reduced by androgen deprivation, suggesting that regulation of the secretory function by androgen remained in these prostates. Together, the data suggest that androgens may elicit regulatory functions in the prostate via multiple pathways. Thus, $Fgfr2^{cn}$ prostates provide a useful animal model for scrutinizing the molecular mechanisms by which androgens regulate prostate growth, homeostasis and function, and may yield clues as to how advanced-tumor prostate cells escape strict androgen regulation.

MATERIALS AND METHODS

Animals

All animals were housed in the Program of Animal Resources of the Institute of Biosciences and Technology, and were handled in accordance with the principles and procedure of the *Guide for the Care and Use of Laboratory Animals*. All experimental procedures were approved by the Institutional Animal Care and Use Committee. The mice carrying LoxP-flanked *Fgfr2* alleles, the ROSA26 reporter and the NKX3.1 (also known as NKX3-1)-Cre knock-in alleles were bred and genotyped as described (Jin et al., 2003b; Soriano, 1999; Yu et al., 2003). Orchiectomy and prostate regeneration were carried out as described previously (Donjacour and Cunha, 1988; Jin et al., 2003a; Wang et al., 2004). Serum levels of androgens in $Fgfr2^{cn}$ and control littermates were measured with the DSL-400 Androgen Assessment kit (Diagnostic Systems Laboratories, Webster, TX).

Collection of prostate tissues and histology analysis

The urogenital complex was excised from mice at the indicated ages and fixed with 4% paraformaldehyde-PBS solution for 30 minutes. The prostates were then dissected from the urogenital tracks under a stereo microscope, weighted and further fixed for an additional 4 hours (Jin et al., 2003a; Wang et al., 2004). In some cases, when comparisons of individual lobes between mutant and control prostates were needed, each individual lobe was dissected and fixed separately. Fixed tissues were serially dehydrated with ethanol, embedded in paraffin and completely sectioned according to standard procedures. Immunohistochemical analyses were performed on 7 μm paraffin sections mounted on Superfrost/Plus slides (Fisher Scientific, Pittsburgh, PA). The antigens were retrieved by autoclaving in Tris-HCl buffer (pH 10.0) for 5 minutes or as suggested by the manufacturers of the antibodies. The source and concentration of primary antibodies are: mouse anti-cytokeratin 8 (1:15 dilution) from Fitzgerald (Concord, MA); mouse anti-smooth muscle α-actin (1:1 dilution) and mouse anti-PCNA (1:1000 dilution) from Sigma (St Louis, MO); mouse anti-p63 (1:150 dilution) and mouse anti-AR (1:150 dilution) from Santa Cruz (Santa Cruz, CA); rabbit anti-probasin (1:3000 dilution) from the Greenberg laboratory; and rabbit anti-PSP94 (1:2000 dilution) from the Xuan laboratory. Total numbers of stained cells from a minimum of three sections per prostate and at least three prostates per genotype were scored for statistical analyses.

For whole-mount lacZ staining, the urogenital sinuses were lightly fixed with 0.2% glutaraldehyde for 30 minutes and incubated overnight with 1 mg/ml X-Gal at room temperature, as described (Liu et al., 2005). For TUNEL assay, tissues were fixed and sectioned as described above, and the apoptotic cells were detected with the ApopTag Peroxidase In Situ Kit (Chemicon, Temecula, CA).

Micro-dissections of the prostate were performed according to Sugimura (Sugimura et al., 1986a). Briefly, individual ductal networks of the prostate gland were micro-dissected after incubation in 1% collagenase-PBS at 4°C overnight. All micro-dissections were performed under a dissection microscope. Numbers of the main ducts and distal ductal tips were scored for statistical analyses.

Secreted protein analyses

The urogenital complex was excised from the mice as described above, and the prostate was dissected from the urogenital complex in PBS. After being dried with paper towels to remove excessive PBS, the prostate was diced with scissors in 100 μl PBS containing 1 mM PMDF. The PBS-extracted secretory proteins were collected by centrifugation as described (Bhatia-Gaur et al., 1999). The protein concentration of the collected sample was normalized with PBS to a final concentration of 1 mg/ml. Samples equivalent to 25 μg of protein were separated on a 5-20% gradient SDS PAGE, and the secretory proteins were visualized with Coomassie Brilliant Blue staining.

In situ hybridization and reverse transcriptase-PCR

For in situ hybridization, paraffin-embedded tissue sections were rehydrated and digested with protease K for 7 minutes at room temperature. After prehybridization at 70°C for 2 hours, the hybridization was carried out by overnight incubation at 70°C with 0.5 μg/ml digoxigenin-labeled RNA probes specific for the FGFR2IIIB isoform. After being washed four times,

Table 1. Nucleotide sequence of primers (5′-3′)

β-actin	GCACCAAGGTGTGATGGTG and GGATGCCACAGGATTCCATA
BMP4	AGGAGGAGGAGGAAGAGCAG and TGTGATGAGGTGTCCAGGAA
BMP7	ACCTGGGCTTACAGCTCTCTGT and CGGAAGCTGACGTACAGCTCATG
β-catenin	GGTGGACTGCAGAAAATGGT and TCGCTGACTTGGGTCTGTCA
FGF7	GGTGAGAAGACTGTTCTGTC and GTGTGTCCATTTAGCTGATG
FGF10	TGTGCGGAGCTACAATCACC and GATGCATAGGTGTTGTATCC
FGFR2	GGGAAGGAGTTTAAGCAGGAGCAT and CTTCAGGACCTTGAGGTAGGGCAG
FGFR2IIIB	GCACTCGGGGATAAATAGCTC and TGTTACCTGTCTCCGCAG
FGFR2IIIC	AGCTGCCGGTGTTAACACCAC and TGTTACCTGTCTCCGCAG
Foxa1	CCATGAACAGCATGACTGCG and TCGTGATGAGCGAGATGTAGGA
Foxa2	GTGAAGATGGAAGGGCTCGA and AGACTCGGACTCAGGTGAGG
Gapdh	GGTGGAGCCAAAAGGGTCAT and GGCCATCACGCCACAGCTTT
Gli1	GAAGGAATCCGTGTGCCATT and GGATCTGTGTAGCGCTTGGT
Gli2	GGCACCAACCCTTCAGACTA and CTGAGCTGCTCCTGGAGTTG
Gli3	GTCAGCCCTGCGGAATACTA and GGAACCACTTGCTGAAGAGC
HoxB13	GATGTGTTGCCAAGGTGAACA and TGAAACCAGATGGTAATCTGGCG
HoxD13	GCAAGAGCCAAGGAAGTGTC and TCGGTAGACGCACATGTCCG
Nkx3.1	ATTGTTCCGTGTCCCTTGTT and GTTTCTACCAGTTCAGGTGT
Notch1	CCCACTGTGAACTGCCCTAT and CACCCATTGACACACACACA
Ptch1	TCAACCCAGCCGACCCAGATT and CCCTGAAGTGTTCATACATTTGCTTGG
Shh	ACATCCACTGTTCTGTGAAAGCA and TCTCGATCACGTAGAAGACCTTCTTGG
TGF-β1	CTAATGGTGGACCGCAACAA and GTACAACTCCAGTGACGTCA
Wnt1	AAGATCGTCAACCGAGGCTG and CATTTGCACTCTTGGCGCAT

each for 30 minutes, with 0.1×DIG washing buffer at 65°C, specifically bound probes were detected by the alkaline phosphatase-conjugated anti-digoxigenin antibody (Roche, Indianapolis, IN). For reverse transcriptase (RT)-PCR analyses, total RNA was extracted from dorsolateral prostates with the RNeasy Mini Kit (QIAGEN, Valencia, CA). Reverse transcriptions were carried out with SuperScript II (GIBCO-BRL, Life Technologies, Grand Island, NY) and random primers according to protocols provided by the manufacturer. RT-PCR was carried out for 30 and 35 cycles, as indicated, at 94°C for 1 minute, 55°C for 1 minute and 72°C for 1 minute with Taq DNA Polymerase (Promega, Madison, WI) and specific primers listed in Table 1. RT-PCR products were analyzed on 2% agarose gels, and the representing data from at least three repetitive experiments were shown. Real-time RT-PCR analyses were carried out with the SYBR Green JumpStart Taq ReadyMix (Sigma) as suggested by the manufacturer. Relative abundances of mRNA were calculated using the comparative threshold (CT) cycle method and normalized with β-actin as an internal control. Data were the means of three individual experiments.

RESULTS

Tissue-specific disruption of *Fgfr2* in the prostatic epithelium

To determine whether FGFR2 was essential for prostatic development, the LoxP-Cre recombination system was used to conditionally inactivate the *Fgfr2* alleles in epithelial cells of the urogenital sinus at late embryonic stages (E17.5) by crossing mice carrying LoxP-flanked *Fgfr2* (*Fgfr2*^{flox}) alleles (Fig. 1A) (Yu et al., 2003) with those carrying an NKX3.1-Cre knock-in allele (Y.P.H., S. M. Price, Z. Chen, W. A. Banach-Petrosky, C. Abate-Shen and M.M.S., unpublished). Deletion of the sequence for exon 8-10 generated a defective allele encoding a truncated FGFR2 ectodomain, as illustrated in Fig. 1B. These epithelial cells later gave rise to prostate epithelial cells. Mice carrying homozygous *Fgfr2*^{flox} and NKX3.1-Cre alleles were viable, fertile and had no apparent pathology. The prostates of mice carrying homozygous *Fgfr2*^{flox} alleles, or heterozygous *Fgfr2*^{flox} alleles with or without the NKX3.1 knock-in allele, had no noticeable differences in gross tissue morphology and histological structures from that of wild-type mice, and therefore were considered as control prostates, although only homozygous *Fgfr2*^{flox} mice were used as controls in most of the study.

Disruption of the *Fgfr2* gene in the prostate of 3-week-old males was confirmed by PCR analysis for the absence of the LoxP-flanked exons (Fig. 1C). RT-PCR analyses of prostates in 7-day-old *Fgfr2*^{cn} mice with FGFR2IIIB-specific primers showed that expression of FGFR2IIIB was below the detection limit; the same experiments with FGFR2IIIC-specific primers or common primers for both FGFR2IIIB and FGFR2IIIC isoforms showed that expression of FGFR2 was significantly reduced in *Fgfr2*^{cn} prostates (Fig. 1D), indicating that the residual FGFR2 expression was due to expression of the FGFR2IIIC isoform in stromal cells or other minor cell populations. Similar results were derived from 3-week-old prostates (data not shown). Furthermore, in situ hybridization with FGFR2IIIB-specific probes showed that the expression of FGFR2 was diminished in the prostate epithelium at 3 weeks (Fig. 1E). Morphological examination revealed that *Fgfr2*^{cn} mice had a notably smaller prostate compared with wild-type mice. Only small and thin dp and lp lobes were apparent in the *Fgfr2*^{cn} prostates, which were also more transparent than control prostates. Because *Fgfr2*^{cn} dp and lp lobes were small and closely connected, rendering them difficult to separate, the dp and lp lobes were collectively referred to as dlp lobes. Among the 45 *Fgfr2*^{cn} prostates examined at different ages, 42 exhibited only two dlp lobes. As for the remaining three mice, in addition to two dlp lobes, one mouse also had a very small anterior lobe, one had a ventral lobe, and one had two small anterior and one ventral lobe. Subsequent analyses were mostly performed with the dlp lobes.

Disruption of *Fgfr2* alleles in the prostate epithelium inhibited prostatic bud-branching morphogenesis

To visualize better the defects in prostatic development in *Fgfr2*^{cn} mice, the ROSA26 reporter allele (Soriano, 1999) was bred into *Fgfr2*^{flox}/NKX3.1-Cre mice. The disruption of *Fgfr2*^{flox} alleles should occur concurrently with activation of the lacZ reporter by excision of the floxed cassette in ROSA26 alleles. The lower urogenital track was then dissected from embryos and newborn pups for whole-mount staining with X-Gal (Fig. 2A). Because the expression of NKX3.1-Cre is initiated in urogenital sinus epithelial cells that give rise to prostate epitheliums between E17.0-E17.5

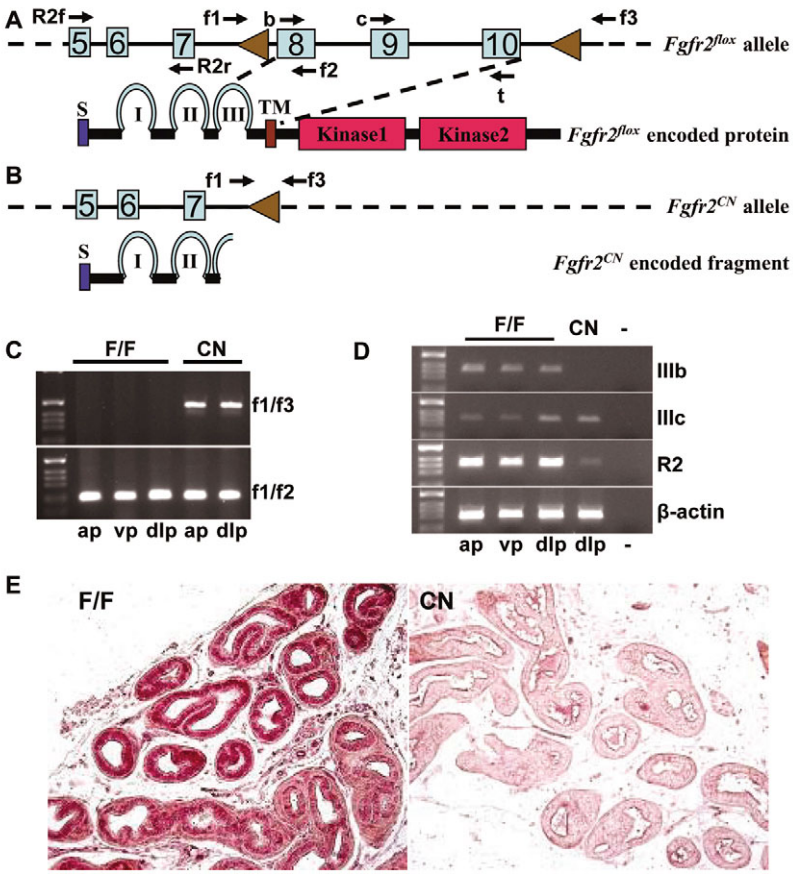

Fig. 1. Disruption of the *Fgfr2* alleles in prostate epithelium. (**A**) Schematic of the floxed *Fgfr2* alleles for conditional disruption. The genomic DNA containing exons 6-10 and the adjacent introns is shown. The primers for PCR genotyping and FGFR2 expression analyses are indicated. (**B**) The $Fgfr2^{cn}$ alleles only encode a truncated ectodomain. (**C**) PCR genotyping. Genomic DNAs extracted from different lobes of $Fgfr2^{cn}$ and control prostates of 3-week-old mice were PCR analyzed with the indicated primers. Primers f1 and f2 amplify a fragment of 207 bp from floxed *Fgfr2* alleles. Primers f1 and f3 amplify a fragment of 471 bp from *Fgfr2*-null alleles, and give no amplification for wild-type *Fgfr2* or $Fgfr2^{flox}$ alleles. (**D**,**E**) Diminished FGFR2 expression in the epithelium of $Fgfr2^{cn}$ prostates. The expression of FGFR2 was assessed with RT-PCR (D) and in situ hybridization (E). Primers R2f and R2r amplify both FGFR2IIIb (IIIb) and FGFR2IIIc (IIIc) isoforms; primers b and t only amplify FGFR2IIIb isoform, primers c and t only amplify FGFR2IIIc isoform. –, negative control without cDNA templates. Panel E shows strong expression of FGFR2 in the epithelial compartment of control prostates, which was diminished in $Fgfr2^{cn}$ prostates. ap, anterior prostate; dlp, dorsolateral prostate; vp, ventral prostate; S, signal peptide; I/II/III, immunoglobulin loop I, II and III, respectively; TM, transmembrane domain; F/F, homozygous $Fgfr2^{flox}$ mice; CN, $Fgfr2^{cn}$ mice.

(Y.P.H., S. M. Price, Z. Chen, W. A. Banach-Petrosky, C. Abate-Shen and M.M.S., unpublished), X-Gal staining was not visible prior to day E17.0, and was only weakly visible at E17.25 in a group of cells surrounding the urethra (data not shown). The staining became more prominent at day E17.5 in cells protruding in different directions, which represent cells giving rise to the prostatic epithelium (Fig. 2A). At this stage, both $Fgfr2^{cn}$ and control embryos developed well-defined ap, dlp and vp buds; no significant difference in X-Gal-staining patterns was observed between $Fgfr2^{cn}$ and control animals. At E18.5, the X-Gal-stained cells in control mice expanded in anterior, dorsolateral and ventral directions (Fig. 2A). By contrast, the same cells in $Fgfr2^{cn}$ mice failed to expand in both anterior and ventral directions, so that the ap and vp buds remained similar to those in E17.5 embryos. Only the cells in dorsal and lateral directions expanded and developed into the dp and lp lobes, respectively. The discrepancy in ap and vp bud formation in $Fgfr2^{cn}$ and control mice became more significant at newborn stages. Only the expanding dlp lobes were visible at P5 (Fig. 2A). To further study the Cre expression pattern, the X-Gal stained tissues were paraffin embedded and sectioned (Fig. 2A, insert; and data not shown). The result showed that expression of lacZ was activated homogenously in the epithelia compartment in every lobe of $Fgfr2^{cn}$ and control prostate, indicating that NKX3.1-Cre efficiently and uniformly excised the silencing cassette in the ROSA26 locus in epithelial cells in every prostatic bud (Fig. 2A). It is expected that the floxed *Fgfr2* alleles were similarly inactivated in all prostatic buds at the same time. Thus, the results imply that FGFR2 signals are more crucial for branching morphogenesis of ap and vp lobes than of dlp lobes, although the underlying molecular mechanism is not clear.

Disruption of *Fgfr2* alleles in prostate epithelium inhibits branching morphogenesis and growth of epithelial ducts

To continue tracking prostate development in $Fgfr2^{cn}$ mice, prostate tissues and the adjacent urethra were dissected from these mice at 2, 4 and 6 weeks of age. Although always smaller and more transparent than normal prostates, $Fgfr2^{cn}$ prostates substantially increased in size during pubertal development (Fig. 2B). The prostate is mainly composed of epithelial ducts packed tightly into a lobular structure. To determine whether the $Fgfr2^{cn}$ prostates had fewer or smaller ducts than control prostates, the dorsolateral lobes of both $Fgfr2^{cn}$ and control prostates were treated with collagenase, and the epithelial ducts were subsequently separated (Fig. 2B′,B″). The number of main ducts and total number of distal ductal tips were then quantified. The results revealed that $Fgfr2^{cn}$ prostates had fewer ducts than the controls. The average number of main ducts in the $Fgfr2^{cn}$ dorsolateral prostates was 7.2, compared with 12.5 in control prostates ($P<0.05$). The average number of distal ductal tips in $Fgfr2^{cn}$ prostates was 58, compared with 113 in control prostates ($P<0.01$). Furthermore, the $Fgfr2^{cn}$ ducts were shorter in length and smaller in diameter than those of the control prostates. This indicates that the disruption of FGFR2 in prostatic bud epithelial cells inhibited both ductal-branching morphogenesis and growth of epithelial ducts.

To investigate whether the FGFR2 kinase was required for rapid growth of prostate cells during pubertal development, proliferating cells in $Fgfr2^{cn}$ and control prostates at the ages of 2, 4 and 6 weeks were assessed by the immunostaining of proliferating cell nuclear antigen (PCNA). At pre-pubertal age (2 weeks), the proliferating cells were mainly localized at the distal tips in both $Fgfr2^{cn}$ and

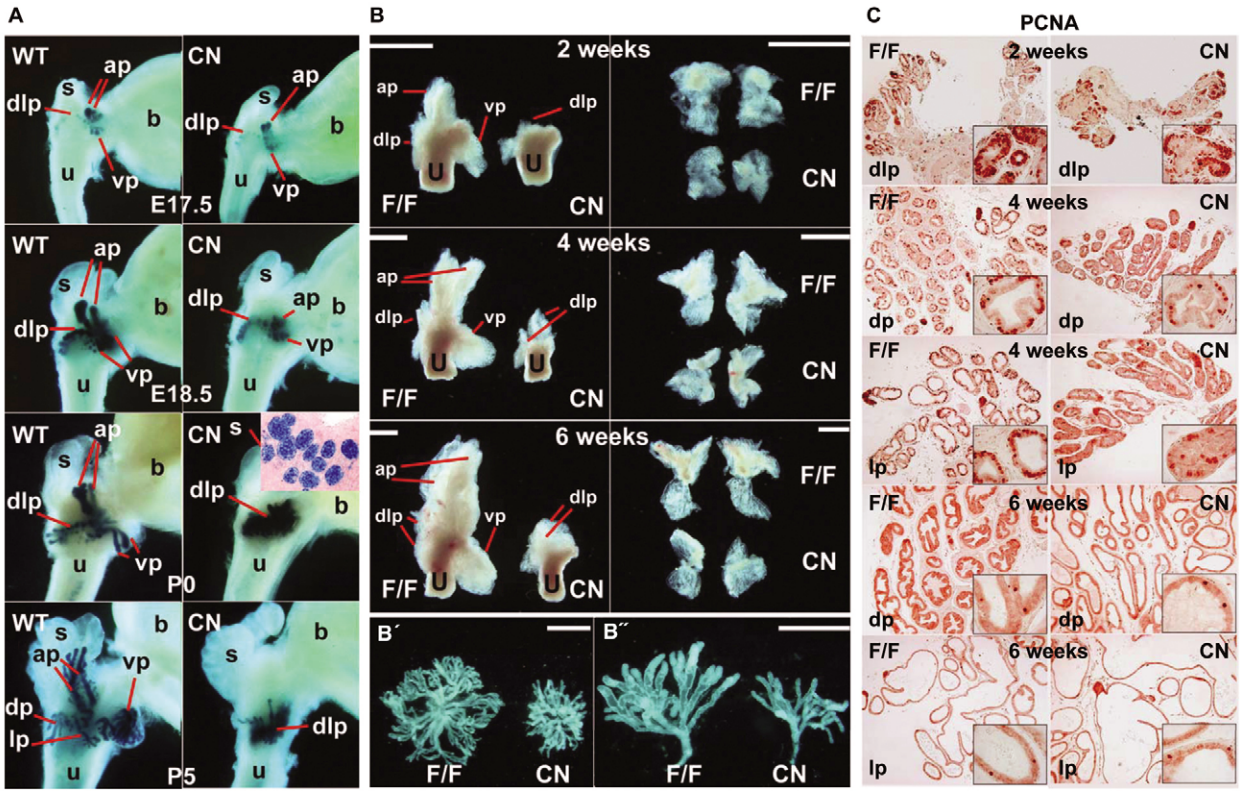

Fig. 2. Disruption of *Fgfr2* alleles leads to perturbed prostate morphogenesis. (**A**) The urogenital sinuses were dissected from embryos or postnatal pups carrying ROSA26/NKX3.1-Cre, and $Fgfr2^{flox}$ or wild-type *Fgfr2* alleles at the indicated days. The tissues were lightly fixed and stained with X-Gal, as described. The stained tissues representing each prostatic lobe are indicated. Notice no significant difference exists in prostatic buds at E17.5 between $Fgfr2^{cn}$ and wild-type controls. Insert: section from the same tissue showing that NKX3.1-Cre efficiently excised the silencing cassette of the ROSA26 allele. (**B**) The prostate and urethra were dissected from mice at the indicated ages (left panels). Right panels: dorsolateral prostate lobes dissected from tissues shown in left panels. (**B′**,**B″**) Epithelial ducts were dissected from dorsolateral prostates of 6-week-old mice with the indicated genotypes. (**C**) The prostate tissues were collected from $Fgfr2^{cn}$ and control mice at the indicated ages, and proliferating cells were identified immunohistochemically by expression of PCNA. Inserts: high-magnification views from the same sections. ap, anterior prostate; dlp, dorsolateral prostate; vp, ventral prostate; u, urethra; b, bladder; s, seminal vesicle; F/F, homozygous $Fgfr2^{flox}$ mice; CN, $Fgfr2^{cn}$ mice. Scar bars: 2 mm.

control prostates (Fig. 2C). Data from three individual prostates showed that approximately 34.2±5.0% of epithelial cells in $Fgfr2^{cn}$ prostates and 36.2±4.4% in control prostates were actively engaged in proliferation. No significant difference was observed at this stage (P>0.05). At the age of 4 weeks, when the mice were undergoing rapid pubertal growth, the proliferating cells were widely distributed in the whole prostate. At this stage, the population of proliferating cells in $Fgfr2^{cn}$ prostates was significantly smaller than that in control prostates (17.8±1.2% in $Fgfr2^{cn}$ prostate and 35.4±3.5% in control prostate, P<0.01). At the post-pubertal age (6 weeks), the proliferating cell population in both $Fgfr2^{cn}$ and control prostates was dramatically reduced (2.00±0.01% in $Fgfr2^{cn}$ prostate and 2.20±0.05% in control prostate, P>0.05), indicating that both $Fgfr2^{cn}$ and control prostates were mature at this stage. Together, the result demonstrates that ablation of *Fgfr2* in prostate epithelium impaired cellular proliferation during pubertal growth.

$Fgfr2^{cn}$ prostates had an underdeveloped epithelium compartment with reduced basal cell population

Epithelial cells in each prostatic lobe normally exhibit a lobe-specific infolding and cellular morphology. Histological analyses showed that $Fgfr2^{cn}$ prostate had less epithelial infolding compared with control prostates, especially in the anterior and dorsolateral lobes (Fig. 3A). The epithelial cells were less polarized with reduced columnarization, suggesting that a deficiency in resident FGFR2 disrupted the completion of terminal differentiation in the epithelium. Notably, among the two adult $Fgfr2^{cn}$ males having poorly developed ap lobes in the prostates (out of 45 $Fgfr2^{cn}$ mice examined), one had two ap lobes that exhibited a tissue structure similar to that of seminal vesicles (Fig. 3A and see Fig. S1 in the supplementary material); the other mouse only had one lobe that had a tissue structure similar to the prostatic bud of newborn mice (data not shown). Nevertheless, semi-quantitative RT-PCR (Fig. 3B) and real-time RT-PCR (Fig. 3C) analyses of total RNA samples extracted from 3-week-old dorsolateral prostates revealed that ablation of *Fgfr2* in the prostate epithelium did not significantly alter the expression of key regulatory molecules for prostate organogenesis and growth, however, the expressions of BMP4, TGF-β and HOXD13 were somewhat reduced in $Fgfr2^{cn}$ prostates. Data from real-time RT-PCR confirmed that the expression of BMP4 in $Fgfr2^{cn}$ prostates was reduced by 55% (P<0.001), TGF-β by 53% (P<0.001) and HOXD13 by 58% (P<0.001). Similar to the data in Fig. 3B, real-time RT-PCR data also showed no significant difference in expression levels of all other tested molecules between $Fgfr2^{cn}$ and control prostates (data not shown).

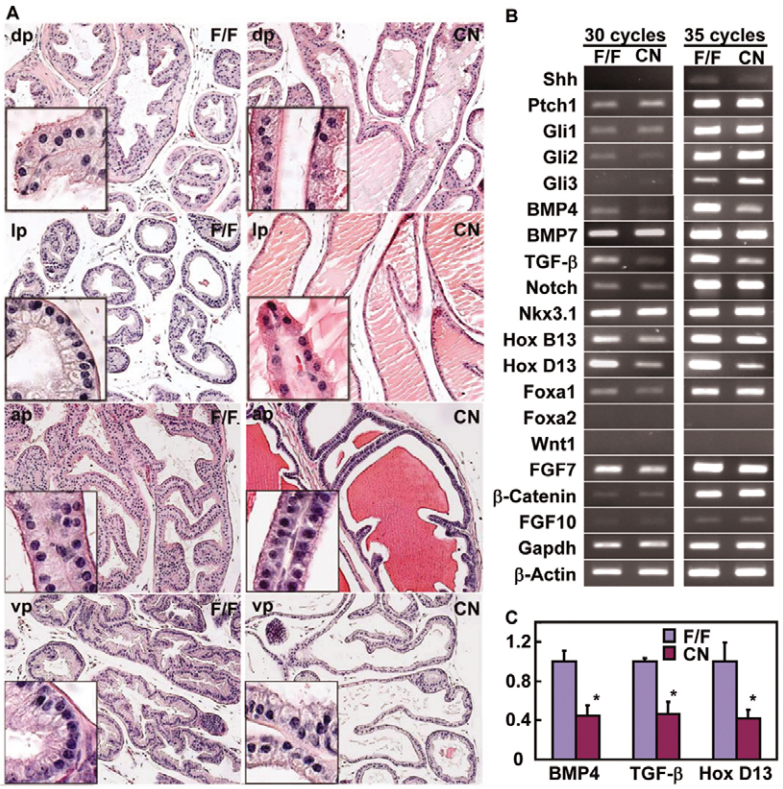

Fig. 3. *Fgfr2^{cn}* prostates exhibited basic prostate characteristics. (**A**) Prostate tissues from 6-week-old mice were sectioned and stained with HE for histological analyses. Inserts: high-magnification views from the same tissues. (**B**) Total RNAs were extracted from dorsolateral prostates of 3-week-old mice and reverse translated with random hexanucleotide primers. RT-PCR was performed as indicated, with β-actin and Gapdh as internal standards. Cycle numbers of amplification are indicated at the top. (**C**) Real-time RT-PCR analyses of the same panel of molecules as in B. Data were normalized with β-actin loading control and were expressed as folds of difference from the control prostates. Data were means of triplicate samples. *P<0.001. F/F, homozygous *Fgfr2^{flox}* mice; CN, *Fgfr2^{cn}* mice; ap, anterior prostate; dp, dorsal prostate; lp, lateral prostate; vp, ventral prostate.

The epithelial compartment of mature prostates mainly consists of well-differentiated luminal epithelial cells that express cytokeratin 8, and basal epithelial cells that express p63 (Cunha et al., 2004; Kurita et al., 2004). The stromal compartment largely consists of smooth muscle cells that express α-actin and are keratin-deficient. To determine whether *Fgfr2^{cn}* prostates also express these characteristic markers, tissue sections were immunochemically analyzed with antibodies against cytokeratin 8, α-actin and p63. The epithelial and stromal cells in *Fgfr2^{cn}* prostates expressed cytokeratin 8 and α-actin, respectively, at levels similar to that seen in control prostates (Fig. 4A).

By contrast, the population of p63-positive basal cells in *Fgfr2^{cn}* prostates was significantly reduced compared with controls, both in growing and mature prostates (Fig. 4B,C). To quantitate the ratio of basal:luminal cells, p63-positive cells in the three sections per prostate were scored. Data from three individual experiments showed that the mean ratios of basal:luminal epithelial cells were 0.48 and 0.67 (P<0.001) in 2-week-old, 0.24 and 0.48 (P<0.001) in 4-week-old, and 0.20 and 0.34 (P<0.001) in 6-week-old *Fgfr2^{cn}* and control prostates, respectively, which validated the observation that the basal cells were reduced in *Fgfr2^{cn}* prostates.

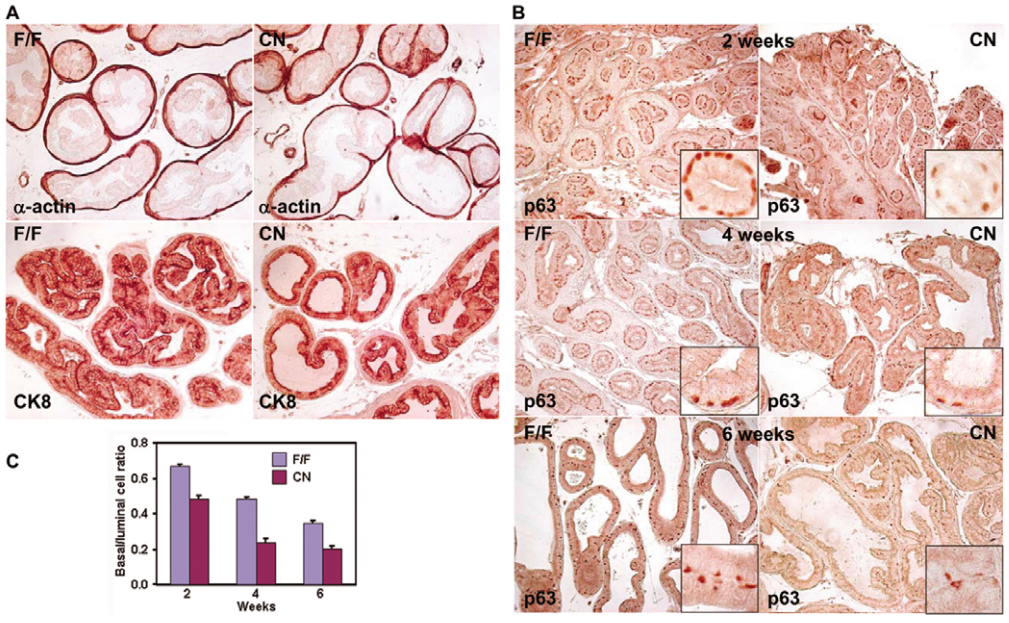

Fig. 4. Immunohistochemical characterization of the *Fgfr2^{cn}* prostate. (**A**) The prostate sections from 4-week-old mice were immunostained with anti-α-actin or anti-cytokeratin 8, as indicated. (**B**) Prostate sections from *Fgfr2^{cn}* and control mice at the indicated ages were immunohistochemically stained with anti-p63 antibodies. Inserts: high-magnification views from the same section. (**C**) Ratios of p63-positive cells in the epithelial compartment were calculated from three samples. Data representing means and s.d. of triplicate samples. F/F, homozygous *Fgfr2^{flox}* mice; CN, *Fgfr2^{cn}* mice.

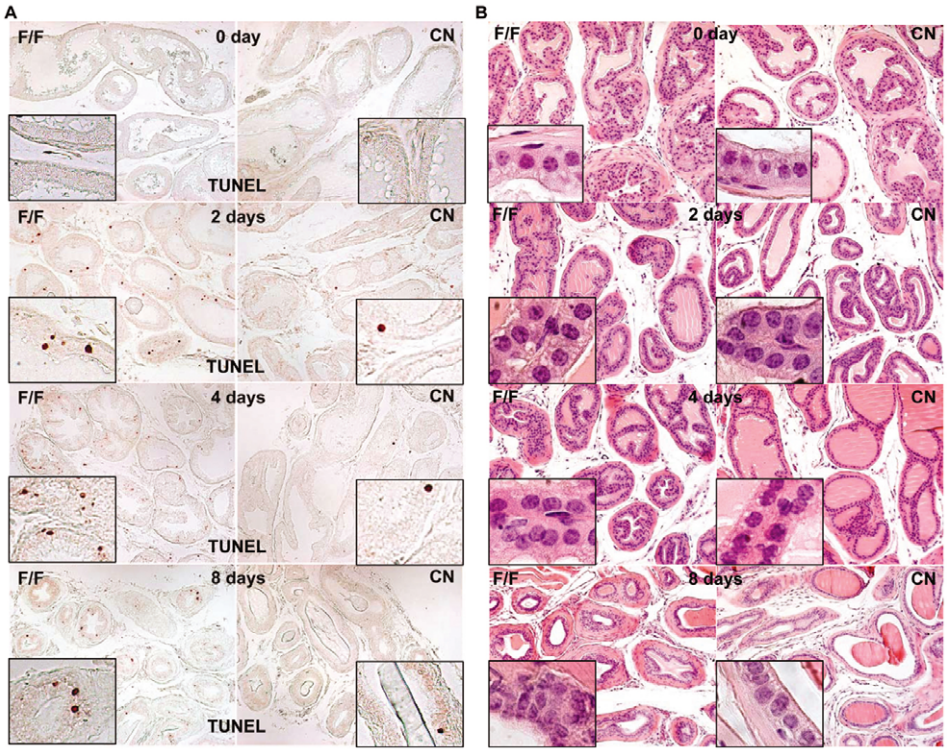

Fig. 5. Diminished androgen dependency in *Fgfr2^{cn}* prostates with respect to tissue homeostasis. (**A**) *Fgfr2^{cn}* and control mice were orchiectomized to eliminate testis-derived androgens. At the indicated day after the operation, the prostate tissues were harvested and apoptotic cells were detected with TUNEL assay. (**B**) HE staining of the same tissues showing that castration failed to induce tissue atrophy in *Fgfr2^{cn}* prostates. F/F, homozygous *Fgfr2^{flox}* mice; CN, *Fgfr2^{cn}* mice.

Ablation of *Fgfr2* diminished androgen dependency with respect to maintenance of tissue homeostasis, but not to production of the secretory proteins in prostates

Androgens are crucial for prostate development, tissue homeostasis and for the production of secretory proteins. To ascertain whether *Fgfr2^{cn}* mice were deficient in androgens, serum androgen levels in *Fgfr2^{cn}* and control littermates were determined. No significant difference in serum androgens was observed. The average androgen concentration in *Fgfr2^{cn}* serum was 7.35±8.00 ng/ml (n=12), and that of control was 8.9±9.1 ng/ml (n=12). Thus, the defect in *Fgfr2^{cn}* prostate development was not a result of androgen insufficiency. To determine whether androgen was required for maintaining tissue homeostasis in *Fgfr2^{cn}* prostates, mice at the age of 6 weeks were orchiectomized to deprive the mice of androgens. Apoptotic cells in the prostates were subsequently assessed with TUNEL analyses (Fig. 5A). The results showed that apoptotic cells were seldom observed in *Fgfr2^{cn}* and control prostates prior to the castration. Apoptotic cells appeared in the epithelial compartment of control prostates within 1 day after castration and became more abundant in days 2-4 post-castration. By sharp contrast, only a limited number of apoptotic cells were detected in the epithelial compartment of *Fgfr2^{cn}* prostates, indicating that the maintenance of cellular homeostasis in *Fgfr2^{cn}* prostates did not depend on androgen as stringently as in control prostates. Hematoxylin and Eosin (HE) staining further demonstrated significant tissue atrophy in the prostate of castrated control, but not the *Fgfr2^{cn}*, males (Fig. 5B).

To investigate whether ARs are expressed similarly in control and *Fgfr2^{cn}* prostates, immunostaining with anti-AR antibodies was carried out. The results revealed that both stromal and epithelial cells in *Fgfr2^{cn}* prostates expressed AR at levels comparable to that detected in control prostates. As in control prostates, the majority of the AR was located in the nucleus of *Fgfr2^{cn}* prostate epithelial cells, indicating no abnormality in

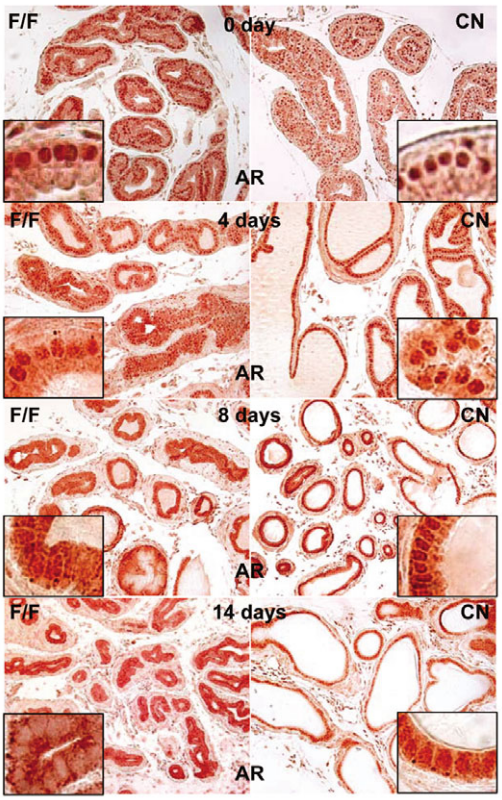

Fig. 6. Expression of the androgen receptor in *Fgfr2^{cn}* prostates. Prostates were harvested from 6-week-old mice before (0 day) and at the indicated days after the castration. Expression and cellular localization of the AR were assessed with immunostaining with anti-AR antibodies. Notice that a considerable amount of AR in *Fgfr2^{cn}* prostates remained in the nuclei at day 14 after the castration. ap, anterior prostate; dp, dorsal prostate; lp, lateral prostate; vp, ventral prostate; F/F, homozygous *Fgfr2^{flox}* mice; CN, *Fgfr2^{cn}* mice.

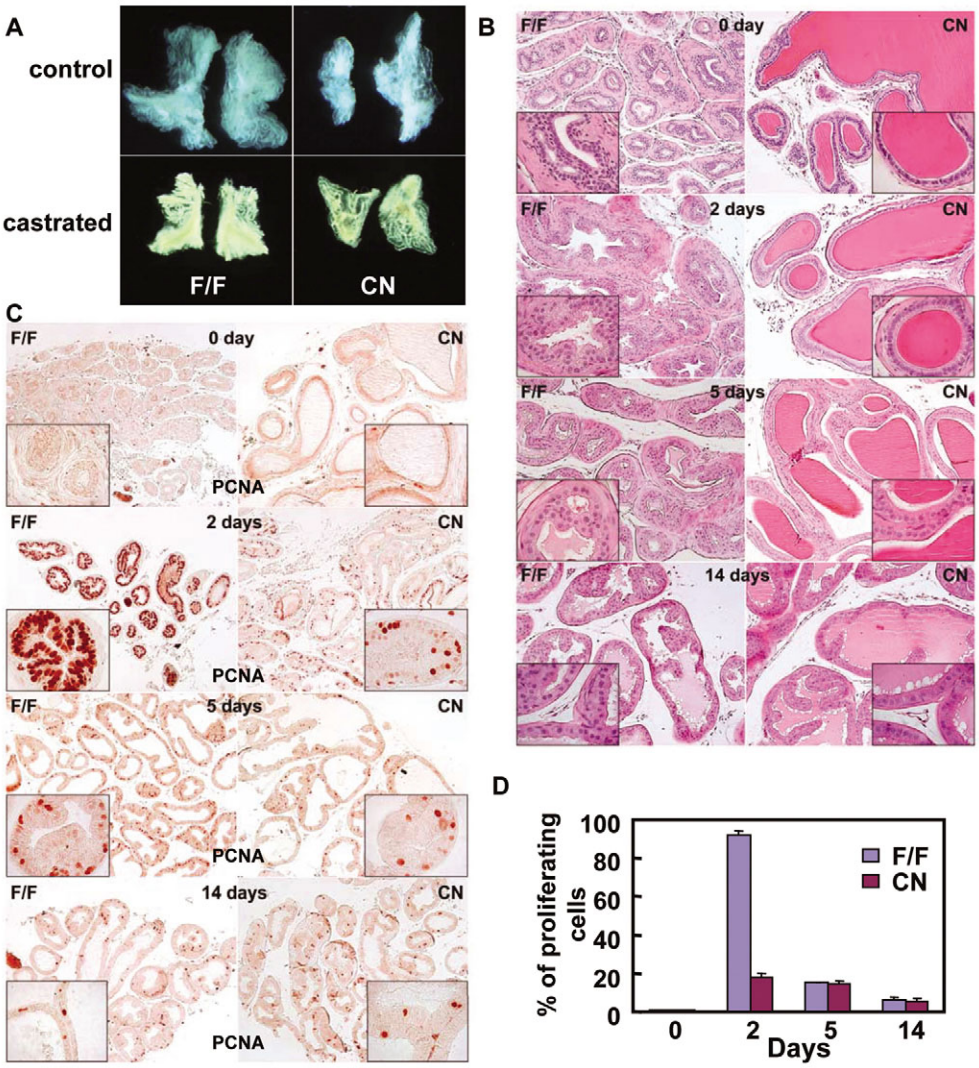

Fig. 7. *Fgfr2^cn^* prostates responded only weakly to androgen replenishment. (**A**) Gross tissue appearance of dorsolateral prostates from *Fgfr2^cn^* and control mice 2 weeks after castration or uncastrated mice at the same age. (**B**) HE staining of dlp dissected from the mice 2 weeks after castration (0 day) and at the indicated days after the androgen replenishment. (**C**) Sections were immunostained with anti-PCNA antibodies to reveal the proliferating cells. Inserts: high-magnification views of the same tissue. (**D**) The mean percentage of PCNA-positive cells in regenerating prostates was calculated from three samples. Data represents means of triplicate samples. CN, *Fgfr2^cn^* mice; F/F, *Fgfr2^flox^* homozygous mice.

either AR expression or nuclear translocation (Fig. 6). To further investigate whether *Fgfr2^cn^* prostates had defects in the subcellular localization of AR after androgen deprivation, prostate sections from castrated control and *Fgfr2^cn^* mice were immunostained with anti-AR antibodies. The results showed that, 14 days after androgen deprivation, most of the AR in control prostates could be found in cytoplasm only (Fig. 6), which is similar to what has previously been reported (Lee and Chang, 2003). However, even 14 days after the castration, a significant amount of AR was still localized in the nucleus of *Fgfr2*-deficient epithelial cells (Fig. 6), which was in sharp contrast to control prostates, which exhibited no nuclear-localized AR at this time point. The prolonged nuclear localization of the AR in *Fgfr2^cn^* prostates may explain why the mutant prostates were less androgen dependent, although the detailed molecular mechanism underlying this phenotype remains to be elucidated.

At 2 weeks after orchiectomy, control prostates underwent tissue atrophy and had a significant change in gross tissue appearance. Consistent with failing to induce apoptosis, androgen deprivation also failed to induce significant tissue morphological changes in *Fgfr2^cn^* prostates (Fig. 7A). HE staining of tissue sections verified that no obvious changes in tissue morphology of *Fgfr2^cn^* prostates could be observed 14 days after the orchiectomy (Fig. 7B). To further examine the effects of androgen in *Fgfr2^cn^* prostates, time-release testosterone pellets were implanted into mice 2 weeks after orchiectomy. The prostates were then harvested from day 1 to day 14 after androgen replenishment for histological analyses. Results showed that androgen replenishment induced massive cellular proliferation in control prostates within 2 days (Fig. 7C,D), and tissue architecture was restored by 2 weeks after the androgen therapy (Fig. 7B), as reported elsewhere (Sugimura et al., 1986b). By contrast, androgen treatment failed to induce significant proliferation in *Fgfr2^cn^* prostates (Fig. 7C,D), a marked contrast to control prostates in which over 90% of luminal epithelial cells were undergoing mitosis at day 2 after androgen treatment. Accordingly, androgen replenishment also failed to induce significant histological changes in *Fgfr2^cn^* prostates (Fig. 7B).

Although budding of the prostate is androgen dependent, prostatic ductal morphogenesis in prenatal and neonatal stages is probably controlled by a combination of chronic androgen stimulation and an intrinsic ‘program’, which, because neonatal castration only impairs approximately 60% of prostatic ductal branching (Donjacour and Cunha, 1988), is not well-defined. To test whether ablation of FGFR2 signaling altered the androgen dependency of neonatal prostatic morphogenesis, neonatal castration was performed on

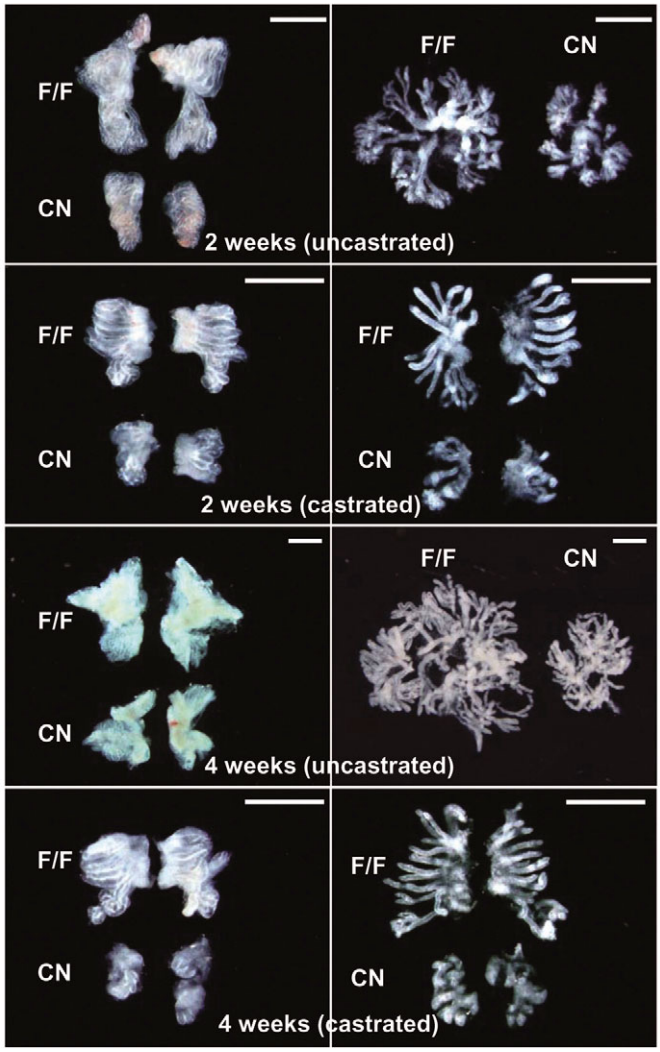

Fig. 8. Prostate development in *Fgfr2^{cn}* and control mice was partially inhibited by neonatal castration. Left panels: gross tissue appearance of prostates from *Fgfr2^{cn}* and control mice at the indicated ages with or without neonatal castration. Right panels: the same tissues were micro-dissected to reveal detailed ductal structures. CN, *Fgfr2^{cn}* mice; F/F, *Fgfr2^{flox}* homozygous mice. Scale bars: 1 mm.

Fgfr2^{cn} and control mice within 24 hours after birth. Results from 2- and 4-week-old neonatally castrated mice showed that the prostate continued to development in both *Fgfr2^{cn}* and control mice, although the size of the dlp lobes was significantly smaller than that of uncastrated counterparts (Fig. 8A). Micro-dissection analyses showed that the differences in complexity of the epithelial ductal network between *Fgfr2^{cn}* and control prostates were not curtailed. Thus, the results indicate that disruption of the FGFR2 signaling axis in the prostatic epithelium does not diminish androgen dependency for neonatal branching morphogenesis or for the pubertal growth of prostates. Together with adult tissue homeostasis data, the result implies divergence in the control of prostatic branching morphogenesis and growth, and of adult prostate tissue homeostasis, by androgens.

A major function of prostates is to produce secretory proteins for semen. HE staining showed that dp and lp lumens of *Fgfr2^{cn}* prostates had abundant eosinophilic substances (Fig. 3A), which probably represent prostatic secretory proteins. SDS-PAGE analyses of PBS-extracts from dlp lumens showed that, as in control prostates, *Fgfr2^{cn}* prostates produced abundant secretory proteins (Fig. 9A). Western blot and real-time RT-PCR showed that *Fgfr2^{cn}* prostates also produced probasin and PSP94 (prostatic secretory protein of 94 amino acids; also known as MSMB – Mouse Genome Informatics), although at reduced levels (Fig. 9B,C). Both probasin and PSP94 are androgen-regulated secretory proteins of dorsolateral prostates in rodents (Huizen et al., 2005; Imasato et al., 2001; Johnson et al., 2000; Kasper and Matusik, 2000).

To clarify whether the secretory function of *Fgfr2^{cn}* prostates is regulated by androgen, prostate secretory proteins were extracted from adult *Fgfr2^{cn}* and control prostates 2 weeks after castration and were analyzed as above. Results showed that the abundance of total soluble proteins (Fig. 9A), and of probasin and PSP94 (Fig. 9B), were significantly reduced in both *Fgfr2^{cn}* and control prostates 2 weeks after castration, even though HE staining showed that the lumen of *Fgfr2^{cn}* prostates was packed with a highly eosinophilic substance. The results suggest that the eosinophilic substances in the prostate of castrated *Fgfr2^{cn}* mice were not PBS-extractable and, therefore, were not normal prostatic secretory proteins. The results showed that, in both control and *Fgfr2^{cn}* prostates, the production of probasin and PSP94, as well as other soluble secretory proteins, was controlled by the androgens. Together, the data indicated that, although ablation of the FGFR2 signaling axis in prostatic epithelium diminished androgen activity in the regulation of homeostasis, it did not abrogate androgen activity in the regulation of secretory-protein production in prostates.

DISCUSSION

Disruption of *Fgfr2* in prostate epithelium impaired prostatic morphogenesis

Despite a large body of indirect evidence, direct demonstration of FGFR2 kinase function in regulating prostatic development, as well as insight into how FGFR2 cross-talks with the androgen signaling axis, has been hampered by its essential role in early embryonic development (De Moerlooze et al., 2000; Xu et al., 1998; Yu et al., 2003). Here, we report that tissue-specific disruption of FGFR2 in prostate epithelium at E17.5 significantly impairs prostatic development. Most *Fgfr2^{cn}* mice developed only two dorsal and two lateral lobes of the prostate instead of the normal eight lobes (two anterior, two dorsal, two lateral and two ventral). Although prostates devoid of FGFR2 in the epithelium retained general prostate-tissue architecture and were active in generating secretory proteins, the epithelial compartment of *Fgfr2^{cn}* prostates had a poorly developed ductal structure characterized by less-extensive intra-ductal infolding, suggesting that the disruption of FGFR2 in the epithelium impaired branching morphogenesis.

The FGF10-FGFR2 signaling axis is important for prostate branching morphogenesis

The finding that ablation of FGFR2 in prostate epithelia significantly inhibits prostate branching morphogenesis is consistent with the notion that FGF10 functions as a mesenchymal paracrine regulator of epithelial growth in the prostate (Thomson and Cunha, 1999). However, prostatic phenotypes in *Fgfr2^{cn}* mice were generally less severe than in *Fgf10*-null mice, because, with a few exceptions that exhibit poorly developed rudimentary prostatic buds, most *Fgf10*-null embryos lack prostatic buds (Donjacour et al., 2003). Furthermore, ex-vivo cultures of *Fgf10*-null urogenital sinus show that *Fgf10*-null phenotypes can not be rescued by FGF10 alone, and

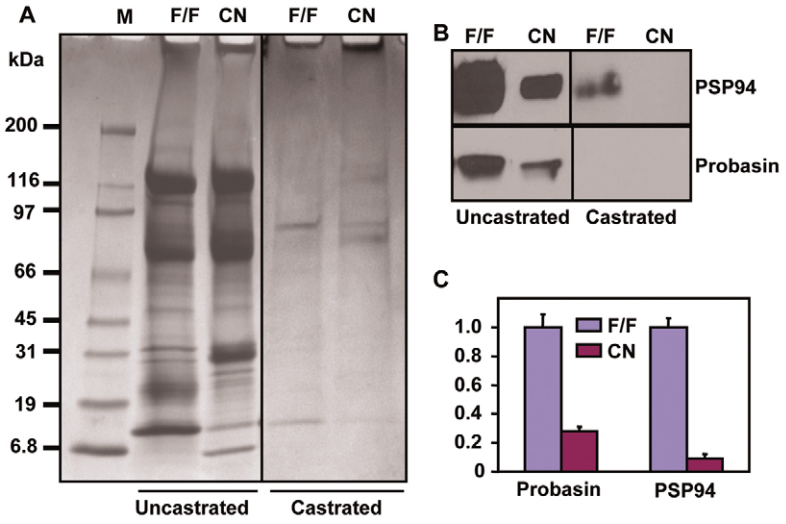

Fig. 9. Production of secretory proteins in *Fgfr2^cn^* prostates remained androgen dependent. (**A**) Profiles of secretory proteins. The PBS-extracted proteins from the dlp of 2-month-old mice were separated on 5-20% gradient SDS-PAGE and stained with Coomassie Brilliant Blue G250. (**B**) Expression of probasin and PSP94 in *Fgfr2^cn^* prostates. The PBS-extracted proteins from castrated or uncastrated mice were separated on SDS-PAGE and were western blotted with anti-probasin and anti-PSP94 antibodies, as indicated. (**C**) Total RNA was extracted from adult *Fgfr2^cn^* and control prostates, and expression of probasin and PSP94 was determined by real-time RT-PCR. Expression levels were normalized to β-actin loading controls. The expression of each gene in control prostates was set to 1. Data are mean±s.d. of three independent experiments. F/F, homozygous *Fgfr2^flox^* mice; CN, *Fgfr2^cn^* mice.

can only be partially rescued by FGF10 together with testosterone, suggesting that FGF10 deficiency may cause other defects as well as those in the epithelial compartment. Thus, the mechanism underlying *Fgf10*-null phenotypes in prostates is not simple. Here, we show that NKX3.1-Cre only efficiently excised floxed sequences in epithelial cells in prostatic rudiments in the urogenital sinus; therefore, the defects in *Fgfr2^cn^* prostates were probably direct phenotypes of a deficiency in FGF10 and/or FGFR2 signals. Thus, *Fgfr2^cn^* prostates provide a good model to assess FGF10 and FGFR2 signaling axis in prostate development and function.

Ablation of *Fgfr2* diminished androgen dependency with respect to tissue homeostasis but not to secretory function

In contrast to adult wild-type prostates, which were stringently androgen dependent, tissue homeostasis in adult *Fgfr2^cn^* prostates was less androgen dependent; androgen deprivation failed to induce tissue degeneration in adult *Fgfr2^cn^* prostates within 2 weeks. Neonatal prostatic morphogenesis is controlled by both androgen dependent and independent mechanisms (Donjacour and Cunha, 1988). Androgen-independent regulation is probably diminished during development because adult prostates are strictly androgen dependent. Interestingly, ablation of FGFR2 did not alter androgen dependency for neonatal branching morphogenesis and pubertal growth of the prostate. Together, the results suggest that FGFR2 signaling is important not only for prostate organogenesis and growth, but also for the prostate to be developed into a strict androgen-dependent organ with respect to tissue homeostasis. Interestingly, AR expression remained intact in both the epithelial and stromal compartments of *Fgfr2^cn^* prostates, and the androgen signaling axis remained active in controlling secretory-protein production in mutant prostates. Thus, it appears that the androgen signaling axis regulates tissue homeostasis and function through different pathways.

The AR in mesenchymal cells is both essential and sufficient for promoting epithelial branching morphogenesis and growth during prostate development (Cunha et al., 2004). Function of the epithelial AR is not understood, although it has been reported to be required for stromal cell differentiation (Thomson, 2001). Data from our present study suggest that the androgen may regulate tissue homeostasis and the production of secretory protein through different mechanisms; it is also androgens that regulate the secretory function of epithelial cells directly through AR signaling pathways within the cells, and that regulate tissue homeostasis through bidirectional communication between the stromal and epithelial compartments. The stromal AR-mediated signals for prostate development and homeostasis have been proposed to be mediated by paracrine growth factors that have been referred to as andromedins. Although FGF7 and FGF10 are proposed to be candidate andromedins in rat prostate-tumor models (Lu et al., 1999; Yan et al., 1992), and ablation of FGF10 disrupts the development of male secondary sex organs, including the prostate (Donjacour et al., 2003), no evidence shows that the expression of FGF10 is androgen regulated in normal prostates (Thomson, 2001; Thomson and Cunha, 1999). Thus, whether FGF10 functions as an andromedin for prostate development remains unknown. Although this study did not address the andromedin issue, the data here demonstrates that FGFR2 signals are important for prostate to develop into a strictly androgen-dependent organ.

Reduced p63-positive basal cells in the *Fgfr2^cn^* prostate

p63-expressing basal cells are a small population of epithelial cells localized as a discontinuous layer between the luminal epithelial cells and the basement membrane, and which account for approximately 10% of cells in mature prostate epithelium. The prostatic basal compartment has been proposed to consist of a pool of cellular subtypes, including tissue stem cells and transient/amplifying progenitor cells, which give rise to terminally differentiated cells (Lam and Reiter, 2006; Rizzo et al., 2005; Tokar et al., 2005). However, the cell-lineage relationship between luminal and basal cells is unclear because the elimination of basal cells by p63 ablation does not affect neuroendocrine (NE)- and luminal-epithelial cell populations (Kurita et al., 2004). Here, we show that prostate rudiments and growing prostates exhibit a higher ratio of basal:luminal epithelial cells, the population of which was gradually reduced as prostates matured (Fig. 4B). Disruption of the FGFR2 signaling axis in prostates significantly reduced the basal cell population, especially in mature prostates. FGF7 has been suggested to have a negative effect on the maintenance of basal cell properties in cell culture by promoting differentiation (Heer et al., 2006).

However, our results suggest that FGFR2 signaling is most probably essential for maintaining basal cell populations in the prostate. Because NKX3.1-Cre was expressed in both basal and luminal epithelial cells, it is possible that FGFR2 either directly controls the basal cell population and their fate-determination within the cells, or indirectly controls this population through regulatory communications between luminal and basal epithelial cells. Further efforts are needed to address this issue.

Development of dlp is less dependent on FGFR2 signaling

Experiments with the ROSA26 reporter indicated that NKX3.1-Cre was expressed in all buds concomitantly between E17.25 and E17.5, indicative that the *Fgfr2* alleles were ablated in all prostatic buds at the same time. Similar to previous reports (Cunha et al., 2004; Thomson, 2001), data in Fig. 2A show that the buds for each prostatic lobe appeared at E17.5. No significant difference was noticeable between $Fgfr2^{cn}$ and control prostates at this stage. The defects in ap and vp lobe development in $Fgfr2^{cn}$ mice apparently occurred between E17.5 and E18.5. Together with the notion that FGFR2IIIB is expressed from the central to the distal tips of the elongating ducts in every prostatic bud during branching morphogenesis (Huang et al., 2005), the results indicate that the development of ap and vp buds is more FGFR2-signal dependent than dlp buds, and that the function of FGFR2 in rodent prostates is lobe-specific. Future experiments with FGFR2IIIB-isoform-null mice will be carried out to validate this finding. Differential responses to regulatory signals among the prostatic lobes are not uncommon in rodent. For example, treating pregnant females with ligands for aryl hydrocarbon receptors also exhibits a lobe-specific inhibition of prostate branching morphogenesis in mouse (Ko et al., 2002); and ablation of HOXA10 in mice causes partial ap-dlp transformation (Marker et al., 2001; Podlasek et al., 1999).

It appears that, relative to other prostatic lobes, the dlp has more potential to escape from strict regulation by the FGFR2 and androgen signaling axes with respect to growth and tissue homeostasis. With regards to tissue structure, the dlp in rodents is the most similar to the peripheral zone of human prostates, where most prostate cancer arises. Together with the fact that the majority of malignant prostate cancers lose FGFR2 expression and are not androgen responsive (Giri et al., 1999a; Kwabi-Addo et al., 2001; McKeehan et al., 1998; Wang and McKeehan, 2003), and that disruption of the FGFR2 signaling axis has been associated with the progression of prostate lesions in mouse models (Jin et al., 2003a; Polnaszek et al., 2003), the results support a model in which the loss of FGFR2 signaling contributes to the escape from androgen regulation in prostate cancer cells.

Prostate development is orchestrated by multiple signaling pathways, including SHH, Notch, BMPs and FGFs. FGF10 has been shown to regulate the expression of multiple morphoregulatory genes, including SHH, BMP4, BMP7, HOXB13 and NKX3.1 (Huang et al., 2005). Here, we demonstrate that, at the mRNA level in $Fgfr2^{cn}$ prostates, the expression of SHH, BMP7, NKX3.1, Notch, HOXB13, β-catenin, Foxa1, FGF7 and FGF10 was similar to that seen in control prostates; and that of TGF-β, BMP4 and Hox D13 was reduced. NKX3.1-Cre mice carry a Cre knock-in allele that is also null for NKX3.1, which causes slight changes in prostate ductal morphogenesis, as well as in secretory-protein expression, in ap and vp lobes (Y.P.H., S. M. Price, Z. Chen, W. A. Banach-Petrosky, C. Abate-Shen and M.M.S., unpublished). Quantitative RT-PCR results show no significant changes in NKX3.1 expression in the dlp of $Fgfr2^{cn}$ mice, indicating that the abnormalities in prostate organogenesis and androgen dependency were independent of NKX3.1 heterozygosity.

In summary, the FGFR2 tyrosine kinase plays a major role in tissue organogenesis and androgen regulation in prostates. Prostates devoid of epithelial resident FGFR2 responded poorly to androgens with respect to cellular homeostasis. Thus, the results suggest that cross-talk between FGFR2 and androgen signaling axes is important for prostate development, tissue homeostasis and tissue function. These results also provide a hint for how advanced prostate cancer escapes strict regulation by androgens.

We thank Mary Cole and Xinchen Wang for critical reading of the manuscript. The work was supported by Public Health Service Grants DAMD17-03-0014 from the US Department of Defense; NIH-CA96824, NIH-CA84296 (NMG) and NIH-CA115985 (MMS) from the National Cancer Institute; and NIH grants HL076664 and HD39952 to D.M.O.

Supplementary material

Supplementary material for this article is available at
http://dev.biologists.org/cgi/content/full/134/4/723/DC1

References

Bhatia-Gaur, R., Donjacour, A. A., Sciavolino, P. J., Kim, M., Desai, N., Young, P., Norton, C. R., Gridley, T., Cardiff, R. D., Cunha, G. R. et al. (1999). Roles for Nkx3.1 in prostate development and cancer. *Genes Dev.* **13**, 966-977.

Cunha, G. R. (1994). Role of mesenchymal-epithelial interactions in normal and abnormal development of the mammary gland and prostate. *Cancer* **74**, 1030-1044.

Cunha, G. R. (1996). Growth factors as mediators of androgen action during male urogenital development. *Prostate Suppl.* **6**, 22-25.

Cunha, G. R., Hayward, S. W., Dahiya, R. and Foster, B. A. (1996). Smooth muscle-epithelial interactions in normal and neoplastic prostatic development. *Acta Anat. Basel* **155**, 63-72.

Cunha, G. R., Ricke, W., Thomson, A., Marker, P. C., Risbridger, G., Hayward, S. W., Wang, Y. Z., Donjacour, A. A. and Kurita, T. (2004). Hormonal, cellular, and molecular regulation of normal and neoplastic prostatic development. *J. Steroid Biochem. Mol. Biol.* **92**, 221-236.

De Moerlooze, L., Spencer-Dene, B., Revest, J., Hajihosseini, M., Rosewell, I. and Dickson, C. (2000). An important role for the IIIb isoform of fibroblast growth factor receptor 2 (FGFR2) in mesenchymal-epithelial signalling during mouse organogenesis. *Development* **127**, 483-492.

Donjacour, A. A. and Cunha, G. R. (1988). The effect of androgen deprivation on branching morphogenesis in the mouse prostate. *Dev. Biol.* **128**, 1-14.

Donjacour, A. A., Thomson, A. A. and Cunha, G. R. (2003). FGF-10 plays an essential role in the growth of the fetal prostate. *Dev. Biol.* **261**, 39-54.

Dorkin, T. J., Robinson, M. C., Marsh, C., Bjartell, A., Neal, D. E. and Leung, H. Y. (1999). FGF8 over-expression in prostate cancer is associated with decreased patient survival and persists in androgen independent disease. *Oncogene* **18**, 2755-2761.

Giri, D., Ropiquet, F. and Ittmann, M. (1999a). Alterations in expression of basic fibroblast growth factor (FGF) 2 and its receptor FGFR-1 in human prostate cancer. *Clin. Cancer Res.* **5**, 1063-1071.

Giri, D., Ropiquet, F. and Ittmann, M. (1999b). FGF9 is an autocrine and paracrine prostatic growth factor expressed by prostatic stromal cells. *J. Cell. Physiol.* **180**, 53-60.

Gnanapragasam, V. J., Robson, C. N., Neal, D. E. and Leung, H. Y. (2002). Regulation of FGF8 expression by the androgen receptor in human prostate cancer. *Oncogene* **21**, 5069-5080.

Hayward, S. W., Rosen, M. A. and Cunha, G. R. (1997). Stromal-epithelial interactions in the normal and neoplastic prostate. *Br. J. Urol.* **79** Suppl. 2, 18-26.

Hayward, S. W., Haughney, P. C., Rosen, M. A., Greulich, K. M., Weier, H. U., Dahiya, R. and Cunha, G. R. (1998). Interactions between adult human prostatic epithelium and rat urogenital sinus mesenchyme in a tissue recombination model. *Differentiation* **63**, 131-140.

Heer, R., Collins, A. T., Robson, C. N., Shenton, B. K. and Leung, H. Y. (2006). KGF suppresses {alpha}2{beta}1 integrin function and promotes differentiation of the transient amplifying population in human prostatic epithelium. *J. Cell Sci.* **119**, 1416-1424.

Huang, L., Pu, Y., Alam, S., Birch, L. and Prins, G. S. (2005). The role of Fgf10 signaling in branching morphogenesis and gene expression of the rat prostate gland: lobe-specific suppression by neonatal estrogens. *Dev. Biol.* **278**, 396-414.

Huizen, I. V., Wu, G., Moussa, M., Chin, J. L., Fenster, A., Lacefield, J. C., Sakai, H., Greenberg, N. M. and Xuan, J. W. (2005). Establishment of a serum tumor marker for preclinical trials of mouse prostate cancer models. *Clin. Cancer Res.* **11**, 7911-7919.

Imasato, Y., Onita, T., Moussa, M., Sakai, H., Chan, F. L., Koropatnick, J., Chin, J. L. and Xuan, J. W. (2001). Rodent PSP94 gene expression is more specific to the dorsolateral prostate and less sensitive to androgen ablation than probasin. *Endocrinology* **142**, 2138-2146.
Jin, C., McKeehan, K., Guo, W., Jauma, S., Ittmann, M. M., Foster, B., Greenberg, N. M., McKeehan, W. L. and Wang, F. (2003a). Cooperation between ectopic FGFR1 and depression of FGFR2 in induction of prostatic intraepithelial neoplasia in the mouse prostate. *Cancer Res.* **63**, 8784-8790.
Jin, C., McKeehan, K. and Wang, F. (2003b). Transgenic mouse with high Cre recombinase activity in all prostate lobes, seminal vesicle, and ductus deferens. *Prostate* **57**, 160-164.
Jin, C., Wang, F., Wu, X., Yu, C., Luo, Y. and McKeehan, W. L. (2004). Directionally specific paracrine communication mediated by epithelial FGF9 to stromal FGFR3 in two-compartment premalignant prostate tumors. *Cancer Res.* **64**, 4555-4562.
Johnson, M. A., Hernandez, I., Wei, Y. and Greenberg, N. (2000). Isolation and characterization of mouse probasin: An androgen-regulated protein specifically expressed in the differentiated prostate. *Prostate* **43**, 255-262.
Kasper, S. and Matusik, R. J. (2000). Rat probasin: structure and function of an outlier lipocalin. *Biochim. Biophys. Acta* **1482**, 249-258.
Ko, K., Theobald, H. M. and Peterson, R. E. (2002). In utero and lactational exposure to 2,3,7,8-tetrachlorodibenzo-p-dioxin in the C57BL/6J mouse prostate: lobe-specific effects on branching morphogenesis. *Toxicol. Sci.* **70**, 227-237.
Kurita, T., Medina, R. T., Mills, A. A. and Cunha, G. R. (2004). Role of p63 and basal cells in the prostate. *Development* **131**, 4955-4964.
Kwabi-Addo, B., Ropiquet, F., Giri, D. and Ittmann, M. (2001). Alternative splicing of fibroblast growth factor receptors in human prostate cancer. *Prostate* **46**, 163-172.
Lam, J. S. and Reiter, R. E. (2006). Stem cells in prostate and prostate cancer development. *Urol. Oncol.* **24**, 131-140.
Lee, D. K. and Chang, C. (2003). Endocrine mechanisms of disease: expression and degradation of androgen receptor: mechanism and clinical implication. *J. Clin. Endocrinol. Metab.* **88**, 4043-4054.
Liu, W., Selever, J., Murali, D., Sun, X., Brugger, S. M., Ma, L., Schwartz, R. J., Maxson, R., Furuta, Y. and Martin, J. F. (2005). Threshold-specific requirements for Bmp4 in mandibular development. *Dev. Biol.* **283**, 282-293.
Lu, W., Luo, Y., Kan, M. and McKeehan, W. L. (1999). Fibroblast growth factor-10. A second candidate stromal to epithelial cell andromedin in prostate. *J. Biol. Chem.* **274**, 12827-12834.
Marker, P. C., Stephan, J. P., Lee, J., Bald, L., Mather, J. P. and Cunha, G. R. (2001). fucosyltransferase1 and H-type complex carbohydrates modulate epithelial cell proliferation during prostatic branching morphogenesis. *Dev. Biol.* **233**, 95-108.
McIntosh, I., Bellus, G. A. and Jab, E. W. (2000). The pleiotropic effects of fibroblast growth factor receptors in mammalian development. *Cell Struct. Funct.* **25**, 85-96.
McKeehan, W. L., Wang, F. and Kan, M. (1998). The heparan sulfate-fibroblast growth factor family: diversity of structure and function. *Prog. Nucleic Acid Res. Mol. Biol.* **59**, 135-176.
Ornitz, D. M. (2000). FGFs, heparan sulfate and FGFRs: complex interactions essential for development. *BioEssays* **22**, 108-112.
Pirtskhalaishvili, G. and Nelson, J. B. (2000). Endothelium-derived factors as paracrine mediators of prostate cancer progression. *Prostate* **44**, 77-87.
Podlasek, C. A., Seo, R. M., Clemens, J. Q., Ma, L., Maas, R. L. and Bushman, W. (1999). Hoxa-10 deficient male mice exhibit abnormal development of the accessory sex organs. *Dev. Dyn.* **214**, 1-12.
Polnaszek, N., Kwabi-Addo, B., Peterson, L. E., Ozen, M., Greenberg, N. M., Ortega, S., Basilico, C. and Ittmann, M. (2003). Fibroblast growth factor 2 promotes tumor progression in an autochthonous mouse model of prostate cancer. *Cancer Res.* **63**, 5754-5760.
Polnaszek, N., Kwabi-Addo, B., Wang, J. and Ittmann, M. (2004). FGF17 is an autocrine prostatic epithelial growth factor and is upregulated in benign prostatic hyperplasia. *Prostate* **60**, 18-24.
Powers, C. J., McLeskey, S. W. and Wellstein, A. (2000). Fibroblast growth factors, their receptors and signaling. *Endocr. Relat. Cancer* **7**, 165-197.
Rizzo, S., Attard, G. and Hudson, D. L. (2005). Prostate epithelial stem cells. *Cell Prolif.* **38**, 363-374.
Ropiquet, F., Giri, D., Lamb, D. J. and Ittmann, M. (1999). FGF7 and FGF2 are increased in benign prostatic hyperplasia and are associated with increased proliferation. *J. Urol.* **162**, 595-599.
Ropiquet, F., Giri, D., Kwabi-Addo, B., Mansukhani, A. and Ittmann, M. (2000). Increased expression of fibroblast growth factor 6 in human prostatic intraepithelial neoplasia and prostate cancer. *Cancer Res.* **60**, 4245-4250.
Song, Z., Wu, X., Powell, W. C., Cardiff, R. D., Cohen, M. B., Tin, R. T., Matusik, R. J., Miller, G. J. and Roy-Burman, P. (2002). Fibroblast growth factor 8 isoform B overexpression in prostate epithelium: a new mouse model for prostatic intraepithelial neoplasia. *Cancer Res.* **62**, 5096-5105.
Soriano, P. (1999). Generalized lacZ expression with the ROSA26 Cre reporter strain. *Nat. Genet.* **21**, 70-71.
Sugimura, Y., Cunha, G. R. and Donjacour, A. A. (1986a). Morphogenesis of ductal networks in the mouse prostate. *Biol. Reprod.* **34**, 961-971.
Sugimura, Y., Cunha, G. R. and Donjacour, A. A. (1986b). Morphological and histological study of castration-induced degeneration and androgen-induced regeneration in the mouse prostate. *Biol. Reprod.* **34**, 973-983.
Thomson, A. A. (2001). Role of androgens and fibroblast growth factors in prostatic development. *Reproduction* **121**, 187-195.
Thomson, A. A. and Cunha, G. R. (1999). Prostatic growth and development are regulated by FGF10. *Development* **126**, 3693-3701.
Tokar, E. J., Ancrile, B. B., Cunha, G. R. and Webber, M. M. (2005). Stem/progenitor and intermediate cell types and the origin of human prostate cancer. *Differentiation* **73**, 463-473.
Wang, F. and McKeehan, W. L. (2003). The fibroblast growth factor (FGF) signaling complex. In *Handbook of Cell Signaling*. Vol. 1 (ed. R. Bradshaw and E. Dennis), pp. 265-270. New York: Academic/Elsevier Press.
Wang, F., McKeehan, K., Yu, C., Ittmann, M. and McKeehan, W. L. (2004). Chronic activity of ectopic type 1 fibroblast growth factor receptor tyrosine kinase in prostate epithelium results in hyperplasia accompanied by intraepithelial neoplasia. *Prostate* **58**, 1-12.
Wang, Q., Stamp, G. W., Powell, S., Abel, P., Laniado, M., Mahony, C., Lalani, E. N. and Waxman, J. (1999). Correlation between androgen receptor expression and FGF8 mRNA levels in patients with prostate cancer and benign prostatic hypertrophy. *J. Clin. Pathol.* **52**, 29-34.
Xu, X., Weinstein, M., Li, C., Naski, M., Cohen, R. I., Ornitz, D. M., Leder, P. and Deng, C. (1998). Fibroblast growth factor receptor 2 (FGFR2)-mediated reciprocal regulation loop between FGF8 and FGF10 is essential for limb induction. *Development* **125**, 753-765.
Yan, G., Fukabori, Y., Nikolaropoulos, S., Wang, F. and McKeehan, W. L. (1992). Heparin-binding keratinocyte growth factor is a candidate stromal-to-epithelial-cell andromedin. *Mol. Endocrinol.* **6**, 2123-2128.
Yu, K., Xu, J., Liu, Z., Sosic, D., Shao, J., Olson, E. N., Towler, D. A. and Ornitz, D. M. (2003). Conditional inactivation of FGF receptor 2 reveals an essential role for FGF signaling in the regulation of osteoblast function and bone growth. *Development* **130**, 3063-3074.